

Elsevier Editorial System(tm) for Advances in Space Research  
Manuscript Draft

Manuscript Number: ASR-D-14-00164R1

Title: The calculation of ionospheric absorption with modern computers

Article Type: Earth magnetosphere and Upper Atmosphere

Keywords: Appleton-Hartree formula; more refined quasi-longitudinal approximation; usually employed non-deviative absorption; Booker's rule.

Corresponding Author: Dr. Alessandro Settimi, Ph.D

Corresponding Author's Institution: Istituto Nazionale di Geofisica e Vulcanologia (INGV)

First Author: Carlo Scotto, Senior Researcher

Order of Authors: Carlo Scotto, Senior Researcher; Alessandro Settimi, Ph.D

Abstract: New outcomes are proposed for ionospheric absorption starting from the Appleton-Hartree formula, in its complete form. The range of applicability is discussed for the approximate formulae, which are usually employed in the calculation of non-deviative absorption coefficient. These results were achieved by performing a more refined approximation that is valid under quasi-longitudinal (QL) propagation conditions. The more refined QL approximation and the usually employed non-deviative absorption are compared with that derived from a complete formulation. Their expressions, nothing complicated, can usefully be implemented in a software program running on modern computers. Moreover, the importance of considering Booker's rule is highlighted. A radio link of ground range  $D = 1000$  km was also simulated using ray tracing for a sample daytime ionosphere. Finally, some estimations of the integrated absorption for the radio link considered are provided for different frequencies.

Response to Reviewers:

Dear Advances in Space Research Co-Editor, Dr. Jan Laštovicka,  
this cover letter is for re-submitting our manuscript (ASR-D-14-00164),

“The calculation of ionospheric absorption with modern computers”,

by the Authors,

Carlo Scotto, Alessandro Settimi.

Please let me know of your decision at your earliest convenience.

Moreover, we would like thanking the Reviewers 1 and 2 for their useful suggestions. We re-wrote several sentences of the paper in order to avoid misunderstandings. We tried to change the paper in all the points that the Reviewers have suggested. We have provided a detailed explanation in the attached reply letters.

Finally, the Reviewers will notice that, in revised manuscript, the minor (or major) revisions occur in words and phrases highlighted by a green-yellow (or red-blue) colour.

With my best regards,

Sincerely yours,

Alessandro Settimi, PhD.

**Reviewer #1:** The authors present a new approximation of the Appleton-Hartree radio wave refractive index to estimate non-deviative absorption. They provide a good introduction into the classical A-H theory and its generalization by Sen and Wyller as well as by Budden.

The derived non-deviative approximation of the absorption coefficient is compared with the complete A-H formulation and its quasi-longitudinal approximation. The application of the non-deviative approximation in ray path calculations results in large differences compared to the other formulations. The manuscript in its present form does not explain explicitly under what conditions the proposed approximations will provide results comparable with the complete A-H formulation and its quasi-longitudinal approximation.

**Authors:** We agree with the Reviewer. This (major) comment was included throughout the manuscript by some lines highlighted in a yellow colour.

**Page 13:** “Only if  $X \ll 1$  ( $\omega \ll \omega_p$ ), when the ray wave is assumed in propagation conditions, away from the reflection, then  $k_{\text{ord}} = k_{\text{ord-long}} = k_{\text{ord-long[NoDev]}$ , i.e. general formulation, a more refined QL approximation and the usually employed non-deviative absorption provide similar values for the local absorption coefficient”.

[See also pages 3, 15: ...](#)

### **Specific comments**

**P1, L 44/45:** The sentence is misleading - if so correct no need would exist for this study since the complete formulation is easy to implement.

**Authors:** This (minor) comment was included throughout the manuscript by some lines highlighted in a green colour.

**Page 1:** “The more refined QL approximation and the usually employed non-deviative absorption are compared with that derived from a complete formulation. Their expressions, nothing complicated, can usefully be implemented in a software program running on modern computers”.

[See also pages 4, 15: ...](#)

**P5 , L 43:** More detailed information are missing how a potential user can obtain appropriate data of the effective collision frequency using the monoenergetic collision frequency as defined on P4, L43. The presentation of a formula would be desirable.

**Authors:** This (major) comment was included throughout the manuscript by some lines highlighted in a yellow colour.

**Page 5:** “Detailed information about data of the pressure can be obtained using the global climatology of atmospheric parameters from the Committee on Space Research (COSPAR) International Reference Atmosphere (CIRA-86) project. As recommended by the COSPAR, the CIRA-86 provides empirical models of atmospheric temperatures and densities. A global climatology of atmospheric temperature, zonal velocity and geopotential height was derived from a combination of satellite, radiosonde and ground-based measurements (Rees, 1988; Rees et al., 1990; Keating, 1996). The reference atmosphere extends from pole to pole and 0-120 km. CIRA-86 consists of tables of the monthly mean values of temperature and zonal wind with almost global coverage (80°N - 80°S). Two files were compiled by Fleming et al. (1988), one in pressure coordinates including also the geopotential heights, and one in height coordinates including also the pressure values”.

**Page 6:** Equation (2) and following comments.

**See also page 11:** ...

**P9/10, section 5:** The description of the computation of radio wave absorption for a model ionosphere is insufficient: any information about the use of collision frequency is missing, the use of a flat earth propagation geometry is highly questionable. The propagation along the magnetic meridian is an optimum choice for the proposed approximation but the differences between the proposed approximation and the other two models are still large.

**Authors:** This (major) comment was included throughout the manuscript by some lines highlighted in a red colour.

**Page 4:** “Moreover, in this paper, an eikonal based ray tracing procedure was used to evaluate the ray path linking two sites 1000 km apart. Some limitations were imposed for simplifying the ray tracing computation. Azzarone et al. (2012) and Settimi et al. (2013, 2014) have already

overcome these limitations, applying the more elaborate Haselgrove's (1955) ray theory and the Jones and Stephenson's (1975) method for ray tracing, which takes into account even the curvature of Earth's surface, and that the ionospheric medium can be characterized by large horizontal gradients.

Finally, in the paper, it is proved our ultimate purpose of underlining that, at any rate in some practical applications, the more refined QL approximation can be used, while the usually employed non-deviative absorption can lead to significant errors in the estimation of absorption. The expression of such QL approximation, nothing complicated, can usefully be implemented in a software program running on modern computers”.

**Pages 11-12:** “... Some limitations were imposed for simplifying the ray tracing computation. Firstly, if the curvature of Earth's surface is ignored, then the flat earth geometry can be applied for wave propagation ...”.

**Page 13-14:** “...The ray paths were assumed to be lying along the magnetic meridian. The wave propagation along the magnetic meridian is an optimum choice just for highlighting how much are even large the differences between the general formulation, the more refined QL approximation and the usually employed non-deviative absorption ...”.

**See also pages 1, 2, 22:** ...

**The quality of figures 1 to 4** is not sufficient for a publication.

**Authors:** All the new figures were attached as tiff files of 300 dpi resolution.

**Figs. 3 and 4:** The  $x$ -axis label is missing.

**Authors:** The  $X=(\omega_p/\omega)^2$  symbol was inserted as the  $x$ -axis label.

**Reviewer #2:** The authors give the example of the calculation of the absorption using electron density profiles calculated from the global model of the ionosphere IRI for high solar activity conditions. Have such calculations for low solar activity? If so, is it possible to add data to the results in this article?

**Authors:** We agree with the Reviewer. This (major) comment was included throughout the manuscript by some lines highlighted in a blue colour.

The calculation of absorption was performed for both low and high solar activity conditions. An old bug has been fixed, so that now the new simulations are correctly computing old and new data results.

**Page 11:** “The June 15 at 12.00 local time (LT) was taken as the input parameter for the IRI and CIRA-86 models, assuming either a low ( $R_{12} = 10$ ) or a high ( $R_{12} = 100$ ) solar activity level, where  $R_{12}$  is the monthly smoothed sunspot number”.

**Page 13:** “The ray paths computed for a 1000 km radio link, at different frequencies, are plotted in Fig. 5”, and following comments ...

**Page 14:** “The corresponding absorption computed for the same 1000 km radio link, at different frequencies, is shown in Fig. 6”, and following comments ...

[See also pages 21-22: ...](#)

## REVIEW

Manuscript Number: ASR-D-14-00164

Title: The calculation of ionospheric absorption with modern computers

Article Type: EM

### P. 4

Line 38 “ $v$ ” replaced by “ $v$ ” (“italic”)

Line 43 “ $s^{-1} \cdot N^{-1}$ ” replaced by “ $s^{-1} \cdot N^{-1}$ ”

Line 56 “ $v$ ” replaced by “ $v$ ” (“italic”)

### P. 5

in formula (1) “ $\rho_N$ ” replaced by “ $\rho_N$ ”

Line 21 “ $v$ ” replaced by “ $v$ ” (“italic”)

### P. 6

in formula (3) “-” replaced by “-”

Line 37 “with” replaced by “where”

Line 40 “ $\omega_p$ ” replaced by “ $\omega_p$ ”

Line 43 “ $\varepsilon_0$ ” replaced by “ $\varepsilon_0$ ”

Line 48 “ $Y_T$ ” and “ $Y_L$ ” replaced by “ $Y_T$ ” and “ $Y_L$ ” (like in formula (5))

Line 56 “ $v/\omega$ ” replaced by “ $v/\omega$ ” (“italic”)

Line 58 in  $n_{\text{ord}} = \dots$  and  $n_{\text{ext}} = \dots$  “-” replaced by “-”

### P. 7

Line 9 “ $v$ ” replaced by “ $v$ ” (“italic”)

Line 12 “ $v$ ” replaced by “ $v$ ” (“italic”)

Line 12 “ $Y_L \dots Y$ ” replaced by “ $Y_L \dots Y$ ”

### P.10

Line 9 requires a reference to IRI model

Line 9 “15 of June at 12.00” replaced by “June 15 at 12.00”

Line 26 in expression for  $B$  “-” replaced by “-”

Line 26 “Tesla” replaced by “T”

Line 46 “ $Y_T$ ” and “ $Y_L$ ” replaced by “ $Y_T$ ” and “ $Y_L$ ”

Line 48 “ $v = 105 \text{ s}^{-1}$ ” replaced by “ $v = 105 \text{ s}^{-1}$ ”

### **P. 11**

Line 19 “-” replaced by “-”

### **P. 12**

Line 31 “ $\chi$ ” replaced by “ $\chi$ ” (“italic”)

### **P. 16**

In captions for Fig. 1 – 4 “ $\text{s}^{-1}$ ” replaced by “ $\text{s}^{-1}$ ”

In Figure 5 are required notations on the axes

**Authors:** All these (minor) comments were included throughout the manuscript by some signs/numbers/symbols highlighted in a green colour.



## Highlights

- New outcomes for ionospheric absorption from the Appleton-Hartree formula.
- Their expressions can usefully be implemented in a software program.
- The importance of considering Booker's rule is highlighted.
- The integrated absorption for a radio link is provided for different frequencies.

## The calculation of ionospheric absorption with modern computers

Carlo Scotto<sup>a</sup>, Alessandro Settini<sup>a</sup>

<sup>a</sup> *Istituto Nazionale di Geofisica e Vulcanologia, Via di Vigna Murata 605, 00143, Rome, Italy*

First author: email, [carlo.scotto@ingv.it](mailto:carlo.scotto@ingv.it); phone, +390651860330; fax, +390651860397

Corresponding author: email, [alessandro.settini@ingv.it](mailto:alessandro.settini@ingv.it); phone, +390651860719; fax, +390651860397

### Abstract

New outcomes are proposed for ionospheric absorption starting from the Appleton-Hartree formula, in its complete form. The range of applicability is discussed for the approximate formulae, which are usually employed in the calculation of non-deviative absorption coefficient. These results were achieved by performing a more refined approximation that is valid under quasi-longitudinal (QL) propagation conditions. **The more refined QL approximation and the usually employed non-deviative absorption are compared with that derived from a complete formulation. Their expressions, nothing complicated, can usefully be implemented in a software program running on modern computers.** Moreover, the importance of considering Booker's rule is highlighted. A radio link of ground range  **$D = 1000$  km** was also simulated using ray tracing for a sample daytime ionosphere. Finally, some estimations of the integrated absorption for the radio link considered are provided for different frequencies.

1  
2  
3  
4  
5  
6  
7  
8  
9  
10  
11  
12  
13  
14  
15  
16  
17  
18  
19  
20  
21  
22  
23  
24  
25  
26  
27  
28  
29  
30  
31  
32  
33  
34  
35  
36  
37  
38  
39  
40  
41  
42  
43  
44  
45  
46  
47  
48  
49  
50  
51  
52  
53  
54  
55  
56  
57  
58  
59  
60  
61  
62  
63  
64  
65

**Keywords:**

Appleton-Hartree formula; more refined quasi-longitudinal approximation; usually employed non-deviative absorption; Booker’s rule.

**1. Introduction**

When the ionospheric radio sounding technique was developed, the first recorded ionograms showed variations in amplitude of the received signal. It was immediately evident that ionospheric absorption occurred at lower altitudes, below those at which the electron density was sufficient to give rise to reflection (Pillet, 1960). Initially it was assumed that this absorption took place in the E region, and several studies were carried out, recording the amplitude of waves reflected from the F region, for both vertical and oblique incidence (Booker, 1935; White and Brown, 1936).

However, already in 1930, Appleton and Ratcliffe measured echo intensity after reflection from the E region, and concluded that the absorption occurs far below the level of reflection. In this way they discovered the existence of a distinct region, which they named the D region.

There was also significant progress in theoretical studies, including the contribution of Booker (1935). He demonstrated that a radio wave can be absorbed even at a level where the refractive index is slightly different from the unit. In practice, this region corresponded to the D region previously proposed by Appleton and Ratcliffe. Other experimental results confirmed the hypothesis of the existence of the D region, with the absorption properties mentioned above. For example, Farmer and Ratcliffe (1935) found a sharp increase in the reflection coefficient during the evening hours, which was attributed to the decreasing absorption coefficient in the D region at dusk.

1  
2  
3  
4 Ever since the first formulation of the magneto-ionic theory, which is controversially  
5 attributed to Appleton and Ratcliffe (1930), or Lassen (1926), it was clear that collisions between  
6 electrons and neutral molecules influenced the local absorption coefficient of radio waves.  
7  
8

9  
10  
11 The magneto-ionic theory, in principle, allowed direct derivation of the local absorption coefficients  
12 for both the ordinary and the extraordinary, while also taking into account the presence of the  
13 magnetic field and collisions. These details can be studied by referring to the well known early  
14 publications of Ratcliffe (1959) and Budden (1961).  
15  
16

17  
18  
19 However, the formulae that can be derived are complicated and difficult to interpret. The focus of  
20 interest was therefore an approximate formula, which will be discussed in the following sections.  
21  
22

23  
24 This takes into account that, in most cases propagation takes place in QL approximation, and for  
25 non-deviative absorption  $\mu \approx 1$  can be assumed,  $\mu$  being the real part of the refractive index  $n$ . It was  
26 thus not considered necessary to substantially revise the theory of non-deviative absorption.  
27  
28

29  
30  
31 In high frequency (HF) radio propagation, the application of the approximate formula has also been  
32 proposed in recent studies, to assess for example the state of the D and E regions by establishing the  
33 local absorption coefficients of the ordinary and extraordinary components of radio waves, and  
34 making use of space-based facilities (Zuev and Nagorskiy, 2012). The effects of HF absorption in  
35 the ionosphere of Mars were also numerically simulated using the same approximate formula  
36 (Withers, 2011; Varun et al., 2012).  
37  
38

39  
40  
41 In the present paper, it is proposed that this mode of operation is no longer justified in all the  
42 applications, like for example riometry. A typical frequency used with this technique is 30 MHz,  
43 with which absorption changes of about 0.1 dB can be measured. **Instead, it is preferable to use the**  
44 **exact formulation or even a more refined QL approximation for all the applications designed in the**  
45 **HF band, such that  $\omega \gg \omega_p$ ,  $\omega$  being the angular frequency of the radio wave considered and  $\omega_p$**   
46 **the plasma frequency.**  
47  
48

1  
2  
3  
4  
5  
6  
7  
8  
9  
10  
11  
12  
13  
14  
15  
16  
17  
18  
19  
20  
21  
22  
23  
24  
25  
26  
27  
28  
29  
30  
31  
32  
33  
34  
35  
36  
37  
38  
39  
40  
41  
42  
43  
44  
45  
46  
47  
48  
49  
50  
51  
52  
53  
54  
55  
56  
57  
58  
59  
60  
61  
62  
63  
64  
65

Moreover, in this paper, an eikonal based ray tracing procedure was used to evaluate the ray path linking two sites 1000 km apart. Some limitations were imposed for simplifying the ray tracing computation. Azzarone et al. (2012) and Settimi et al. (2013, 2014) have already overcome these limitations, applying the more elaborate Haselgrove’s (1955) ray theory and the Jones and Stephenson’s (1975) method for ray tracing, which takes into account even the curvature of Earth’s surface, and that the ionospheric medium can be characterized by large horizontal gradients. Finally, in the paper, it is proved our ultimate purpose of underlining that, at any rate in some practical applications, the more refined QL approximation can be used, while the usually employed non-deviative absorption can lead to significant errors in the estimation of absorption. The expression of such QL approximation, nothing complicated, can usefully be implemented in a software program running on modern computers.

**2. The classical and generalized magneto-ionic theories**

In the initial formulation of magneto-ionic theory, a frictional term is utilized that does not depend on the root-mean-square electron velocity and the electron velocity distribution. It represents a first approximation of the effective collision frequency due to the collisions between electrons and neutrals. Later, several studies were published that strived to improve this aspect of the theory. Originally, Phelps and Pack (1959) measured the collision cross-section  $\sigma$  for electrons in the nitrogen N<sub>2</sub> — the most abundant atmospheric constituent up to 100 km — establishing that it is proportional to the root-mean-square electron velocity  $v_{rms}$ . Consequently, Sen and Wyller (1960) generalized the Appleton-Hartree magneto-ionic theory including a Maxwellian velocity distribution of the electrons (a), and extending the findings of Phelps and Pack (1959) to all constituents of air (b). However, Sen and Wyller (1960) made several key mistakes, later remedied

1  
2  
3  
4 by Manchester (1965). A valuable approximation of the generalized magneto-ionic theory exists in  
5  
6 Flood (1980).

7  
8  
9 The momentum collision frequency  $\nu$  of electrons with neutrals can be simply expressed by the  
10  
11 product of pressure  $p$  times a constant  $\alpha$ . Based on both laboratory and ionospheric data  $\alpha$  can be  
12  
13 estimated as  $\alpha = 6.41 \cdot 10^5 \text{ m}^2 \cdot \text{s}^{-1} \cdot \text{N}^{-1}$  (Thrane and Piggott, 1966; Friedrich and Torkar, 1983; Singer  
14  
15 et al., 2011).

16  
17  
18  
19 Detailed information about data of the pressure can be obtained using the global climatology of  
20  
21 atmospheric parameters from the Committee on Space Research (COSPAR) International Reference  
22  
23 Atmosphere (CIRA-86) project. As recommended by the COSPAR, the CIRA-86 provides  
24  
25 empirical models of atmospheric temperatures and densities. A global climatology of atmospheric  
26  
27 temperature, zonal velocity and geopotential height was derived from a combination of satellite,  
28  
29 radiosonde and ground-based measurements (Rees, 1988; Rees et al., 1990; Keating, 1996). The  
30  
31 reference atmosphere extends from pole to pole and 0-120 km. CIRA-86 consists of tables of the  
32  
33 monthly mean values of temperature and zonal wind with almost global coverage (80°N - 80°S).  
34  
35 Two files were compiled by Fleming et al. (1988), one in pressure coordinates including also the  
36  
37 geopotential heights, and one in height coordinates including also the pressure values.

38  
39  
40  
41  
42  
43 The atmosphere in the E and D layers consists mainly of nitrogen  $\text{N}_2$  (about 78%), with  
44  
45 atomic and molecular oxygen  $\text{O}_2$  as the next most important constituents. The relatively large cross  
46  
47 section for  $\text{N}_2$  makes it likely, as a first-order approximation, that the height variation of collision  
48  
49 frequency  $\nu$  is proportional to the partial pressure of the  $\text{N}_2$ . Experiments show that the cross section  
50  
51 for  $\text{O}_2$  also varies by the square root of  $T$  so that the two contributions can be combined (Davies,  
52  
53 1990).

54  
55  
56  
57  
58 When there is complete mixing of the atmospheric gases the following relationship holds:  
59  
60  
61

$$\frac{dp}{p} = \frac{d\rho_N}{\rho_N} + \frac{dT}{T} = -\frac{dH}{H}, \quad (1)$$

where  $p$  is the total pressure,  $\rho_N$  the number density,  $T$  the absolute temperature of molecules, and  $H = k_B T / mg$  the atmospheric scale height, with  $g$  the gravity acceleration and  $m$  the mean molecular mass. For this reason, the collision frequency  $\nu$  varies by the height  $h$  above ground as (Thrane and Piggott, 1966):

$$\nu(h) = \nu_0 \frac{p(h)}{p_0}. \quad (2)$$

Theoretically, a decreasing exponential law holds in an atmosphere which is constant in composition (Budden, 1961):  $\nu(h) = \nu_0 \exp[-(h-h_0)/H]$ , where  $\nu_0$  is a constant, i.e.  $\nu_0 = \nu(h_0)$ , and  $h_0$  is the height corresponding to the maximum electron density  $N_0$ , i.e.  $N_0 = N(h_0)$ . On equal terms, this maximum occurs for a null solar zenith angle  $\chi$ , i.e.  $\chi = 0$ . In practice,  $H$  takes different values at different levels, and the law can only be expected to hold over ranges of  $h$  so small that  $H$  may be treated as constant. Experimentally, in the thermosphere (above about 100 km) CIRA-86 is identical with the Mass-Spectrometer-Incoherent-Scatter (MSIS-86) model (Hedin, 1987). In the lower part of thermosphere (at 120 km altitude) CIRA-86 was merged with MSIS-86.

According to Budden (1965), while the generalized theory (Sen and Wyller, 1960) is important in the detailed quantitative interpretation of certain experiments, for most practical radio propagation problems the classical theory (Appleton and Chapman, 1932) is adequate, especially when appropriate values are used for the effective collision frequency.

### 3. Absorption theory in general formulation

It is known that, in general, the integral absorption of a radio wave through the ionosphere can be described in differential form by the exponential decrease in the field amplitude  $E$ , which can be expressed using a relationship of the type:

$$E(s) = E_0 \cdot \exp(-k \cdot s), \quad (3)$$

$s$  being the curvilinear abscissa along the ray path, and  $k$  the local absorption coefficient. This can be expressed by the following relation:

$$k = \omega \cdot \chi / c, \quad (4)$$

where  $\chi$  is the imaginary part of complex refractive index  $n = \mu - i\chi$  and  $c$  is the velocity of light.

Both  $\mu$  and  $\chi$  can be derived from the Appleton-Hartree equation:

$$n_{\text{ord, ext}}^2 = 1 - \frac{X}{1 - iZ - \frac{1}{2} \frac{Y_T^2}{(1 - X - iZ)} \pm \sqrt{4(1 - X - iZ)^2 + Y_L^2}}, \quad (5)$$

where:

$X = \omega_p^2 / \omega^2$  (where  $\omega$  is the angular frequency of the radio wave,  $\omega_p = \sqrt{Ne^2 / m\epsilon_0}$  the plasma frequency,  $N$  the profile of electron density,  $m$  the electron mass,  $e$  the electron charge, and  $\epsilon_0$  the constant permittivity of vacuum);



1  
2  
3  
4  $Y_{\parallel} = Y \cdot \sin(\theta)$ ,  $Y_{\perp} = Y \cdot \cos(\theta)$  (where  $\theta$  is the angle between the wave vector and the Earth's  
5  
6 magnetic field), and  $Y = \omega_B / \omega$  ( $\omega_B = Be/m$  being the gyro-frequency, and  $B$  the amplitude of the  
7  
8 Earth's magnetic field);  
9

10  
11  $Z = \nu / \omega$  (where  $\nu$  is the collision frequency).  
12  
13

14 This equation gives two indices of refraction  $n_{\text{ord}} = \mu_{\text{ord}} \pm i \cdot \chi_{\text{ord}}$  and  $n_{\text{ext}} = \mu_{\text{ext}} \pm i \cdot \chi_{\text{ext}}$  for the  
15 known birefringence of ionospheric plasma. The two refractive indices are obtained from Eq. (5)  
16 through the choice of positive or negative signs, which must be decided applying the so-called  
17 Booker's rule. Once the critical frequency is defined  $\omega_c = (\omega_B/2) \cdot \sin^2(\theta) / \cos(\theta)$ , this rule states that,  
18 to achieve continuity of  $\mu_{\text{ord}}$  ( $\mu_{\text{ext}}$ ) and  $\chi_{\text{ord}}$  ( $\chi_{\text{ext}}$ ), if  $\omega_c / \nu > 1$ , the positive (negative) sign in Eq. (5)  
19 must be adopted both for  $X < 1$  and for  $X > 1$ ; while, if  $\omega_c / \nu < 1$ , the positive (negative) sign for  $X$   
20  $< 1$  and negative (positive) for  $X > 1$  must be adopted.  
21  
22  
23  
24  
25  
26  
27  
28  
29  
30

31 It is clearly not a simple task to analytically derive  $\mu_{\text{ord}}$  ( $\mu_{\text{ext}}$ ) and  $\chi_{\text{ord}}$  ( $\chi_{\text{ext}}$ ) from Eq. (5). However,  
32 this is facilitated by some commercial mathematical software tool packages able to  
33 perform symbolic computation. Using those tools, it is easy to obtain analytical expressions for  $\mu_{\text{ord}}$   
34 ( $\mu_{\text{ext}}$ ) and  $\chi_{\text{ord}}$  ( $\chi_{\text{ext}}$ ), which are extremely complicated, difficult to interpret, and not worth reporting,  
35 but nevertheless providing relationships that can be effectively and easily introduced into  
36 calculation algorithms.  
37  
38  
39  
40  
41  
42  
43  
44

45 Moreover, from  $\chi_{\text{ord}}$  and  $\chi_{\text{ext}}$ , applying Eq. (4), gives  $k_{\text{ord}}$  and  $k_{\text{ext}}$ , with obvious symbol meanings.  
46  
47  
48  
49  
50

#### 51 **4. The theory of non-deviative absorption** 52 53 54 55

56 If the QL propagation approximation is assumed to be valid, it holds that:  
57  
58  
59  
60  
61  
62  
63  
64  
65

$$\frac{Y_r^4}{4 \cdot [(1-X)^2 + Z^2]} \ll Y_L^2. \quad (6)$$

From this relationship, considering that:

$$Z \ll 1, \quad (7)$$

then  $\theta \ll 1 \rightarrow Y_L \cong Y$  and Eq. (5) can be reduced to the simplified form:

$$n_{\text{ord-long,ext-long}}^2 = (\mu_{\text{ord-long,ext-long}} - i\chi_{\text{ord-long,ext-long}})^2 = 1 - \frac{X}{1 - iZ \pm Y}. \quad (8)$$

Once some mathematical steps have been performed, Eq. (8) is split into two equations, one for the real part,

$$\mu_{\text{ord-long,ext-long}}^2 - \chi_{\text{ord-long,ext-long}}^2 \cong \mu_{\text{ord-long,ext-long}}^2 = 1 - \frac{X(1 \pm Y)}{(1 \pm Y)^2 + Z^2}, \quad (9)$$

and one for the imaginary part,

$$2\mu_{\text{ord-long,ext-long}} \cdot \chi_{\text{ord-long,ext-long}} = \frac{X \cdot Z}{(1 \pm Y)^2 + Z^2}. \quad (10)$$

Under the simplifying condition  $\mu \ll \chi$ , once the real part  $\mu$  of the refractive index is calculated from Eq. (9), the imaginary part  $\chi$  of the refractive index can be derived from Eq. (10), by a simple passage, obtaining:

$$\chi_{\text{ord-long,ext-long}} = \frac{1}{2\mu_{\text{ord-long,ext-long}}} \frac{X \cdot Z}{(1 \pm Y)^2 + Z^2}. \quad (11)$$

This relation, by introducing Eq. (4), gives:

$$k_{\text{ord-long,ext-long}} = \frac{1}{2\mu_{\text{ord-long,ext-long}}} \frac{Ne^2}{c m \varepsilon_0} \frac{\nu}{(\omega \pm \omega_B)^2 + \nu^2}. \quad (12)$$

It is obvious that this formula is used in practice only assuming (in non-deviative absorption approximation):  $\mu_{\text{ord-long}} \approx 1$  ( $\mu_{\text{ext-long}} \approx 1$ ). The local absorption coefficient, which is obtained from Eq. (12) by replacing  $\mu_{\text{ord-long}} \approx 1$  ( $\mu_{\text{ext-long}} \approx 1$ ), will be indicated as  $k_{\text{ord-long[NoDev]}}$ , ( $k_{\text{ext-long[NoDev]}}$ ). The positive sign has to be applied to the ordinary and the negative to the extraordinary. Note that Eq. (12) is valid in QL conditions. In this case, similarly to what happens for longitudinal propagation, Booker's rule should not be considered. If not performing the approximation  $\mu_{\text{ord-long}} \approx 1$  ( $\mu_{\text{ext-long}} \approx 1$ ), from Eq. (8) it is possible to derive relationships for  $\mu_{\text{ord-long}}$  ( $\mu_{\text{ext-long}}$ ) and  $\chi_{\text{ord-long}}$  ( $\chi_{\text{ext-long}}$ ). In this case complicated expressions are obtained, difficult to interpret and not worth reporting. Besides, applying  $\chi_{\text{ord-long}}$  ( $\chi_{\text{ext-long}}$ ) it is possible to compute  $k_{\text{ord-long}}$  ( $k_{\text{ext-long}}$ ) through Eq. (4).

As is explained clearly in Ratcliffe's well known early publication (1959), in a very wide range of  $\omega$ ,  $\nu$ , and  $\theta$ , propagation occurs in QL conditions. In practice, QL conditions are always

1  
2  
3  
4 verified, except for  $X \sim 1$ . Eq. (12), considering  $\mu \approx 1$ , is therefore often used to calculate the non-  
5  
6 deviative absorption coefficients of the ordinary and extraordinary rays except when  $X \sim 1$ , for  
7  
8 example, for frequencies  $\omega \gg \omega_p$  ( $X \ll 1$ ).  
9  
10

11 A better approximation for  $k$ , also limited to the case of QL conditions, can be derived using Eq.  
12  
13 (8), and deducing from this  $\chi_{\text{ord-long}}$  (and  $\mu_{\text{ord-long}}$ ), from which  $k$  can be derived using Eq. (4). In this  
14  
15 case, complicated expressions are obtained, difficult to interpret, and not worth reporting, but that  
16  
17 can usefully be incorporated inside commercial mathematical software tool packages.  
18  
19  
20  
21  
22  
23

## 24 **5. The computation of absorption in a modelled ionosphere**

25  
26  
27  
28

29 It is interesting to make further comparisons of full equations with approximations using  
30  
31 well-known literature models of electron density and collision frequency. For practical applications,  
32  
33 radio wave absorption can be expressed in decibels (dB). As an example, a numerical simulation  
34  
35 calculates the output of absorption, having as inputs: an electron density  $N$  obtained from the  
36  
37 International Reference Ionosphere (IRI) model (Bilitza, 1990; Bilitza and Reinisch, 2008), and a  
38  
39 collision frequency  $\nu$  proportional to the pressure data obtained from the CIRA-86 model. The June  
40  
41 15 at 12.00 local time (LT) was taken as the input parameter for the IRI and CIRA-86 models,  
42  
43 assuming either a low ( $R_{12} = 10$ ) or a high ( $R_{12} = 100$ ) solar activity level, where  $R_{12}$  is the monthly  
44  
45 smoothed sunspot number. Basing on these  $N$  and  $\nu$  models, an eikonal based ray tracing procedure  
46  
47 was used to evaluate the ray path linking two sites 1000 km apart. Some limitations were imposed  
48  
49 for simplifying the ray tracing computation. Firstly, if the curvature of Earth's surface is ignored,  
50  
51 then the flat earth geometry can be applied for wave propagation. Secondly, if the ionospheric  
52  
53 medium is characterized by small horizontal gradients, then the azimuth angle of transmission can  
54  
55 be assumed to be a constant along the great circle path (Davies, 1990). All the more, considering a  
56  
57  
58  
59  
60  
61  
62  
63  
64  
65

1  
2  
3  
4 flat layering ionosphere, so without any horizontal gradient, the profiles of electron density  $N(h)$   
5  
6 and collision frequency  $\nu(h)$  are assumed to be functions only of the height. At the limit, a single  
7  
8 profile for both  $N(h)$  and  $\nu(h)$  recurs throughout the latitude and longitude grid of points involved in  
9  
10 the ray tracing computation.  
11  
12  
13  
14

## 15 16 **6. Results and discussion**

17  
18  
19  
20  
21 In Fig. 1(a)-(d),  $\mu_{\text{ord}}$  e  $\mu_{\text{ord-long}}$  ( $\mu_{\text{ext}}$  e  $\mu_{\text{ext-long}}$ ) are reported for different values of the  $\theta$  angle,  
22  
23 having considered a radio wave with  $Y = (Y_1^2 + Y_2^2)^{1/2} = 0.5$ , frequency  $f = 4$  MHz, and a minimal  
24  
25 collision frequency  $\nu = 10^5 \text{ s}^{-1}$ , typical of the high D region around an altitude of 90 km, which  
26  
27 maximises the absorption variances among the general formulation, QL, and non-deviative  
28  
29 approximations. The curves are shown with different colours, as indicated in the figure legend. In  
30  
31 essence, it demonstrates the possibility of approximating  $\mu_{\text{ord}}$  with  $\mu_{\text{ord-long}}$  and  $\mu_{\text{ext}}$  with  $\mu_{\text{ext-long}}$ , as  
32  
33 long as conditions do not require changing sign for  $X = 1$ , as specified in Booker's rule. This fact is  
34  
35 reflected in the similar curves  $\chi_{\text{ord}}$  and  $\chi_{\text{ord-long}}$  ( $\chi_{\text{ext}}$  and  $\chi_{\text{ext-long}}$ ), which are shown in Fig. 2 (a)-(d). In  
36  
37 fact, when Eq. (5) is approximated to Eq. (8) an assumption more limiting than QL conditions is  
38  
39 made, considering the propagation as perfectly longitudinal. Now, to study the propagation, it is  
40  
41 particularly important to investigate the conditions for which  $\mu = 0$ , when ionospheric reflection  
42  
43 takes place. In this regard, it is known that, in the absence of collisions, even a small value of the  $\theta$   
44  
45 angle is sufficient to ensure that the ordinary ray has critical frequency of reflection for  $X = 1$  and  
46  
47 the extraordinary for  $X = 1 \pm Y$ . Only for  $\theta = 0$  is the ordinary ray reflected in  $X = 1 + Y$  and the  
48  
49 extraordinary in  $X = 1 - Y$ . In other words, in the absence of collisions, it is only for  $\theta = 0$  that  
50  
51 propagation can be considered, with good reason, to be perfectly longitudinal. Effectively, in the  
52  
53 presence of collisions, if the condition  $X \sim 1$  is not verified, propagation occurs in QL conditions.  
54  
55  
56  
57  
58  
59  
60  
61  
62  
63  
64  
65

1  
2  
3  
4 However, the same reflection conditions of perfectly longitudinal propagation occur only if:  $\omega_c/\nu <$   
5  
6 1. This can be verified by observing the graphs of  $\mu_{\text{ord}}$  and  $\mu_{\text{ord-long}}$  ( $\mu_{\text{ext}}$  and  $\mu_{\text{ext-long}}$ ) [Fig. 1 (a) - (d)].  
7  
8 The same behaviour is observed in the graphs of  $\chi_{\text{ord}}$  and  $\chi_{\text{ord-long}}$  ( $\chi_{\text{ext}}$  and  $\chi_{\text{ext-long}}$ ) [Fig. 2 (a) - (d)].  
9  
10 Therefore, even if the range of QL conditions is very wide, the possibility of considering  
11 propagation to be perfectly longitudinal, and approximating Eq. (5) with Eq. (8), is limited by the  
12 condition  $\omega_c/\nu < 1$ . This is evident in Figs. 3 (d) and 4 (d), where  $\omega_c/\nu > 1$ . These figures show for  
13 example that for  $X \sim 0.5$ ,  $k_{\text{ord}}$  and  $k_{\text{ord-long}}$  deviate appreciably from  $k_{\text{ord-long[NoDev]}}$ . Only if  $X \ll 1$  ( $\omega$   
14  $\ll \omega_p$ ), when the ray wave is assumed in propagation conditions, away from the reflection, then  
15  $k_{\text{ord}} = k_{\text{ord-long}} = k_{\text{ord-long[NoDev]}}$ , i.e. general formulation, a more refined QL approximation and the  
16 usually employed non-deviative absorption provide similar values for the local absorption  
17 coefficient.

18  
19 Generally, the eikonal based ray tracing has to assume the absence of geomagnetic field.  
20  
21 Conversely, the presence of the geomagnetic field has to be considered when computing absorption.  
22  
23 The geomagnetic field was assumed as  $B \approx 4.5 \cdot 10^5$  T. Absorption was computed for the ordinary  
24 ray along the ray paths. The ray paths were assumed to be lying along the magnetic meridian. The  
25 wave propagation along the magnetic meridian is an optimum choice just for highlighting how  
26 much are even large the differences between the general formulation, the more refined QL  
27 approximation and the usually employed non-deviative absorption. The ray paths computed for a  
28 1000 km radio link, at different frequencies, are plotted in Fig. 5. The low ray paths occur in a  
29 narrower HF band (3-11 MHz) assuming low solar activity, and in a wider HF band (2-14 MHz)  
30 assuming high solar activity. The apogee of low ray paths reaches a similar altitude ( $h \approx 100$  km)  
31 for both solar activity levels. Indeed, that altitude corresponds to the bottom of E-layer (reflecting  
32 the low ray paths as a mirror). Instead, the high ray paths occur in the HF band (9-14 MHz),  
33 similarly for both the solar activity levels. The apogee of high ray paths reaches a higher altitude ( $h$

1  
2  
3  
4 > 200 km, throughout the HF band 9-14 MHz) assuming low solar activity, and a lower altitude  
5  
6 (100 <  $h$  < 200 km, especially for lowest HF 9-11 MHz) assuming high solar activity. Indeed, the  
7  
8 F1-layer, which appears for both the solar activity levels, is characterized by a higher critical  
9  
10 plasma frequency assuming high solar activity. The corresponding absorption computed for the  
11  
12 same 1000 km radio link, at different frequencies, is shown in Fig. 6. Firstly, the refined QL  
13  
14 approximation and the usually employed non-deviative approximation provide comparable values  
15  
16 for low ray paths, throughout the whole HF band (2-14 MHz). Indeed, aside from the reflection due  
17  
18 to the bottom of E-layer, the low ray propagation is just non-deviative, such that the real part of  
19  
20 refractive index can be assumed as unitary, i.e.  $\mu = 1$ . Secondly, the refined QL approximation  
21  
22 provides more accurate values than the usually employed non-deviative approximation for high ray  
23  
24 paths, especially for lowest HF 9-11 MHz). Indeed, the high ray propagation in the F1-F2 layers is  
25  
26 even deviative, when that the real part of refractive index must be assumed less than unit, i.e.  $\mu < 1$ .  
27  
28 Thirdly, the refined QL approximation and the usually employed non-deviative approximation  
29  
30 provide underestimates compared to the general formulation, assuming either a low or a high solar  
31  
32 activity, and both the approximations tend to the general formulation, especially for highest HF  
33  
34 (12-14 MHz). Indeed, the general formulation takes into account the deviative and non-deviative  
35  
36 propagations occurring across the E and F1-F2 layers, where the real part of refractive index is  
37  
38 generally assumed as  $\mu \leq 1$ . However, Figs. 5 and 6 prove our ultimate purpose of underlining that,  
39  
40 at any rate in some practical applications, the more refined QL approximation can be used, while  
41  
42 the usually employed non-deviative absorption can lead to significant errors in the estimation of  
43  
44 absorption.  
45  
46  
47  
48  
49  
50  
51  
52  
53  
54  
55  
56  
57  
58  
59  
60  
61  
62  
63  
64  
65

1  
2  
3  
4  
5  
6  
7  
8  
9  
10  
11  
12  
13  
14  
15  
16  
17  
18  
19  
20  
21  
22  
23  
24  
25  
26  
27  
28  
29  
30  
31  
32  
33  
34  
35  
36  
37  
38  
39  
40  
41  
42  
43  
44  
45  
46  
47  
48  
49  
50  
51  
52  
53  
54  
55  
56  
57  
58  
59  
60  
61  
62  
63  
64  
65

## 7. Summary

The main results can be summarized as follows:

- 1) Commercial mathematical software tool packages make it easy to obtain exact values of  $k_{\text{ord}}$  ( $k_{\text{ext}}$ ), which are obtained from  $\chi_{\text{ord}}$  ( $\chi_{\text{ext}}$ ) [Eq. (4)] and applying the Appleton-Hartree formula [Eq. (5)].
- 2) The local absorption coefficient  $k_{\text{ord-long[NoDev]}}$  ( $k_{\text{ext-long[NoDev]}}$ ), calculated by Eq. (12) setting  $\mu_{\text{ord-long[NoDev]}} \approx 1$  ( $\mu_{\text{ext-long[NoDev]}} \approx 1$ ), is an acceptable approximation only for  $X \ll 1$  ( $\omega \ll \omega_p$ ).
- 3) A better approximation for  $k_{\text{ord-long}}$  ( $k_{\text{ext-long}}$ ) can be obtained from  $\chi_{\text{ord-long}}$  ( $\chi_{\text{ext-long}}$ ), which are calculated from Eq. (8) without setting  $\mu_{\text{ord-long[NoDev]}} \approx 1$  ( $\mu_{\text{ext-long[NoDev]}} \approx 1$ ). The expression of such QL approximation, nothing complicated, can usefully be implemented in a software program running on modern computers.
- 4) It is important to consider the application of Booker's rule, applied equally to the calculation of  $\mu$  and  $\chi$ , which is required when calculating ionospheric absorption.



1  
2  
3  
4 **References**  
5  
6  
7  
8

9 Appleton, E. V., and Chapman, F. W., The collisional friction experienced by vibrating electrons in  
10 ionized air, Proc. Phys. Soc. London, 44 (243), 246–254, doi: 10.1088/0959-5309/44/3/302, 1932.  
11  
12  
13

14  
15  
16 Appleton, E. V., and Ratcliffe, J. A., Some simultaneous observations on down coming wireless  
17 waves, Proc. R. Soc. Lond. A, 128 (807), 133–158, doi: 10.1098/rspa.1930.0101, 1930.  
18  
19  
20

21  
22  
23 Azzarone, A., Bianchi, C., Pezzopane, M., Pietrella, M., Scotto, C., and Settimi, A., IONORT: a  
24 Windows software tool to calculate the HF ray tracing in the ionosphere, Comput. Geosci. - UK, 42,  
25 57-63, doi: 10.1016/j.cageo.2012.02.008, 2012.  
26  
27  
28  
29

30  
31  
32  
33 Bilitza, D. (ed.), International Reference Ionosphere (IRI) 1990, National Space Science Data  
34 Center (NSSDC), Report 90-22, Greenbelt, Maryland, 85 pp., 1990.  
35  
36  
37

38  
39  
40 Bilitza, D., and Reinisch, B. W., International Reference Ionosphere 2007: Improvements and new  
41 parameters, Adv. Space Res., 42 (4), 599–609, doi:10.1016/j.asr.2007.07.048, 2008.  
42  
43  
44

45  
46  
47 Booker, H. G., The application of the magnetoionic theory to the ionosphere, Proc. R. Soc. Lond. A,  
48 150 (870), 267–286, doi: 10.1098/rspa.1935.0101, 1935.  
49  
50  
51

52  
53  
54 Budden, K. G., Radio waves in the ionosphere, Cambridge University Press, Cambridge, 688 pp.,  
55 1961.  
56  
57  
58

1  
2  
3  
4  
5  
6  
7  
8  
9  
10  
11  
12  
13  
14  
15  
16  
17  
18  
19  
20  
21  
22  
23  
24  
25  
26  
27  
28  
29  
30  
31  
32  
33  
34  
35  
36  
37  
38  
39  
40  
41  
42  
43  
44  
45  
46  
47  
48  
49  
50  
51  
52  
53  
54  
55  
56  
57  
58  
59  
60  
61  
62  
63  
64  
65

Budden, K. G., Effect of electron collisions on the formulas of magnetoionic theory, Radio Sci., 69D (2), 191-211, <http://archive.org/details/jresv69Dn2p191>, 1965.

Committee on Space Research (COSPAR), The COSPAR International Reference Atmosphere (CIRA-86), NCAS British Atmospheric Data Centre, 2006 (Available from [http://badc.nerc.ac.uk/view/badc.nerc.ac.uk\\_\\_ATOM\\_\\_dataent\\_CIRA](http://badc.nerc.ac.uk/view/badc.nerc.ac.uk__ATOM__dataent_CIRA)).

Davies, K., Ionospheric Radio, Peter Peregrinus Ltd. (ed.) on behalf of the Institution of Electrical Engineers (IET), London, UK, 508 pp., 1990.

Farmer, F. T., and Ratcliffe, J. A., Measurements of the absorption of wireless waves in the ionosphere, Proc. R. Soc. Lond. A, 151 (873), 370–383, doi: 10.1098/rspa.1935.0156, 1935.

Fleming, E. L., Chandra, S., Shoerberl, M. R., and Barnett, J. J., Monthly mean global climatology of temperature, wind, geopotential height and pressure for 0-120 km, National Aeronautics and Space Administration, Technical Memorandum 100697, Washington, D.C., 85 pp., 1988.

Flood, W. A., A D-region mid- and high-latitude approximation to the Sen-Wyller refractive index equations, Radio Sci., 15 (4), 797-799, doi: 10.1029/RS015i004p00797, 1980.

Friedrich, M., and Torkar, K. M., Collision Frequencies in the High-Latitude D-Region, J. Atmos. Terr. Phys., 45 (4), 267-271, doi: 10.1016/S0021-9169(83)80048-8, 1983.

1  
2  
3  
4  
5  
6  
7  
8  
9  
10  
11  
12  
13  
14  
15  
16  
17  
18  
19  
20  
21  
22  
23  
24  
25  
26  
27  
28  
29  
30  
31  
32  
33  
34  
35  
36  
37  
38  
39  
40  
41  
42  
43  
44  
45  
46  
47  
48  
49  
50  
51  
52  
53  
54  
55  
56  
57  
58  
59  
60  
61  
62  
63  
64  
65

Haselgrove, J., Ray theory and a new method of ray tracing, Conference on the Physics of the Ionosphere, Proc. Phys. Soc. London, 23, 355-364, 1955.

Hedin, A. E., MSIS-86 Thermospheric Model, J. Geophys. Res., 92 (A5), 4649–4662, doi:10.1029/JA092iA05p04649, 1987.

Jones, R. M., and Stephenson, J. J., A versatile three-dimensional ray tracing computer program for radio waves in the ionosphere, OT Report, 75-76, U. S. Department of Commerce, Office of Telecommunication, U. S. Government Printing Office, Washington, USA, 185 pp, 1975.

Keating, G. M. (ed.), COSPAR International Reference Atmosphere (CIRA)-1986, Part III: Trace Constituent Reference Models, Adv. Space Res., 18 (9/10), 11-58, doi: 10.1016/0273-1177(96)00050-6, 1996.

Lassen, H. I., Zeitschrift für Hochfrequenztechnik, Volume 28, pp. 109–113, 1926.

Manchester, R., Correction to paper by H.K. Sen and A.A. Wyller "On the generalization of the Appleton-Hartree Magnetoionic Formulas", J. Geophys. Res., 70 (19), 4995, doi: 10.1029/JZ070i019p04995, 1965.

Phelps, A. V., and Pack, J. L., Electron collision frequencies in nitrogen and in the lower ionosphere, Phys. Rev. Lett., 3 (7), 340-342, doi: 10.1103/PhysRevLett.3.340, 1959.

1  
2  
3  
4  
5  
6  
7  
8  
9  
10  
11  
12  
13  
14  
15  
16  
17  
18  
19  
20  
21  
22  
23  
24  
25  
26  
27  
28  
29  
30  
31  
32  
33  
34  
35  
36  
37  
38  
39  
40  
41  
42  
43  
44  
45  
46  
47  
48  
49  
50  
51  
52  
53  
54  
55  
56  
57  
58  
59  
60  
61  
62  
63  
64  
65

Pillet, G., Contribution a l'étude de l'absorption ionosphérique sur une fréquence fixe, Annales des Télécommunications, 15 (7-8), 157-184, doi:10.1007/BF03012072, 1960.

Ratcliffe, J. A., The Magneto-Ionic Theory and its Applications to the Ionosphere, Cambridge University Press, Cambridge, 206 pp., 1959.

Rees, D. (ed.), COSPAR International Reference Atmosphere (CIRA)-1986, Part I: Thermospheric Models, Adv. Space Res., 8 (5/6), 27-106, doi: 10.1016/0273-1177(88)90039-7, 1988.

Rees, D., Barnett, J. J., and Labitzke, K. (ed.), COSPAR International Reference Atmosphere (CIRA)-1986, Part II: Middle Atmosphere Models, Adv. Space Res., 10 (12), 357-517, doi: 10.1016/0273-1177(90)90405-O, 1990.

Sen, H. K., and Wyller, A. A., On the Generalization of the Appleton-Hartree Magnetoionic Formulas, J. Geophys. Res., 65 (12), 3931-3950, doi: 10.1029/JZ065i012p03931, 1960.

Settimi, A., Pezzopane, M., Pietrella, M., Bianchi, C., Scotto, C., Zuccheretti, E., and Makris, J., Testing the IONORT-ISP system: a comparison between synthesized and measured oblique ionograms, Radio Sci., 48 (2), 167-179, doi:10.1002/rds.20018, 2013.

Settimi, A., Pietrella, M., Pezzopane, M., Zolesi, B., Bianchi, C., and Scotto, C., The COMPLEIK subroutine of the IONORT-ISP system for calculating the non-deviative absorption: A comparison with the ICEPAC formula, Adv. Space. Res., 53 (2), 201-218, doi: 10.1016/j.asr.2013.10.035, 2014.

1  
2  
3  
4  
5  
6  
7  
8  
9  
10  
11  
12  
13  
14  
15  
16  
17  
18  
19  
20  
21  
22  
23  
24  
25  
26  
27  
28  
29  
30  
31  
32  
33  
34  
35  
36  
37  
38  
39  
40  
41  
42  
43  
44  
45  
46  
47  
48  
49  
50  
51  
52  
53  
54  
55  
56  
57  
58  
59  
60  
61  
62  
63  
64  
65

Singer, W., Latteck, R., Friedrich, M. Wakabayashi, M., and Rapp, M., Seasonal and solar activity variability of D-region electron density at 69°N, *J. Atmos. Terr. Phys.*, 73 (9), 925-935, doi: 10.1016/j.jastp.2010.09.012, 2011.

Thrane, E. V., and Piggott, W. R., The Collision Frequency in the D- and E-Regions of the ionosphere, *J. Atmos. Terr. Phys.*, 28 (8), 721-737, doi: 10.1016/0021-9169(66)90021-3, 1966.

Varun, S., Haider, S. A., Withers, P., Kozarev, K., Jun, I., Kang, S., Gronoff, G., and Wedlund, C. S., Numerical simulation of the effects of a solar energetic particle event on the ionosphere of Mars, *J. Geophys. Res.*, 117, A05312, doi:10.1029/2011JA017455, 2012.

White, F. W. G., and Brown, L. W., Some measurements of the reflection coefficient of the ionosphere for wireless waves (Mesures du coefficient de réflexion de l'ionosphère pour les ondes radioélectriques), *Proc. R. Soc. Lond. A*, 153 (880), 639–660, doi: 10.1098/rspa.1936.0028, 1936.

Withers, P., Attenuation of radio signals by the ionosphere of Mars: Theoretical development and application to MARSIS observations, *Radio Sci.*, 46 (2), RS2004, doi:10.1029/2010RS004450, 2011.

Zuev, V. V., and Nagorskiy, P. M. Estimation Method of the Ionospheric D region Using Space-Based Radio Facilities, *Izvestiya, Atmospheric and Oceanic Physics*, 48 (9), 879–886, doi:10.1134/S0001433812090186, 2012.

1  
2  
3  
4  
5  
6  
7  
8  
9  
10  
11  
12  
13  
14  
15  
16  
17  
18  
19  
20  
21  
22  
23  
24  
25  
26  
27  
28  
29  
30  
31  
32  
33  
34  
35  
36  
37  
38  
39  
40  
41  
42  
43  
44  
45  
46  
47  
48  
49  
50  
51  
52  
53  
54  
55  
56  
57  
58  
59  
60  
61  
62  
63  
64  
65

**Figure captions**

**Figure 1.** The graphs  $\mu_{ord}$ ,  $\mu_{ord-long}$ ,  $\mu_{ext}$  and  $\mu_{ext-long}$  for different values of the  $\theta$  angle, considering a radio wave with  $Y = 0.5$ , frequency  $f = 4$  MHz, a collision frequency  $\nu = 10^5$  s<sup>-1</sup>. The curves are shown in different colours, as reported in the legend.

**Figure 2.** The graphs  $\chi_{ord}$ ,  $\chi_{ord-long}$ ,  $\chi_{ext}$  and  $\chi_{ext-long}$  for different values of the  $\theta$  angle, considering a radio wave with  $Y = 0.5$ , frequency  $f = 4$  MHz, a collision frequency  $\nu = 10^5$  s<sup>-1</sup>. The curves are shown in different colours, as reported in the legend.

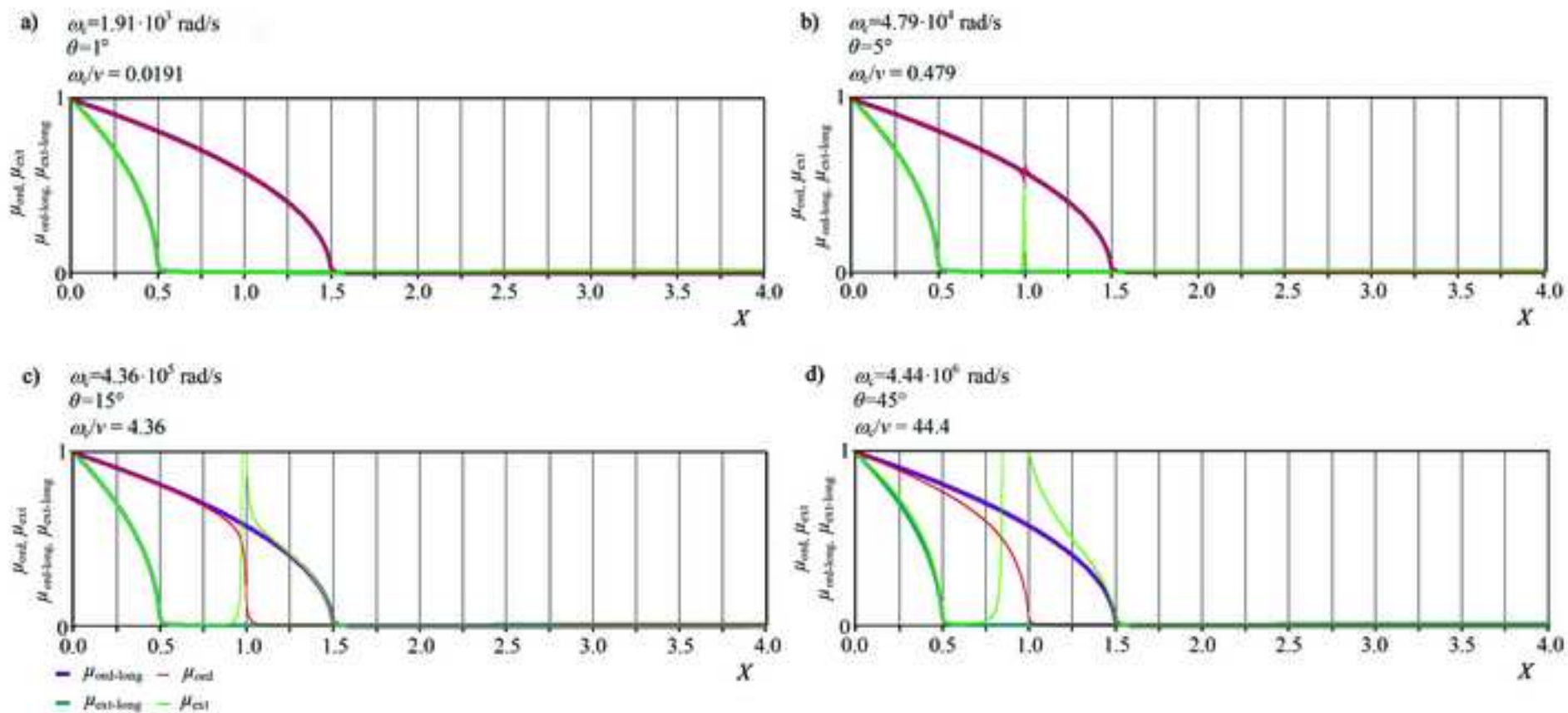
**Figure 3.** The graphs  $k_{ord}$ ,  $k_{ord-long}$  and  $k_{ord-long[NoDev]}$  for different values of the  $\theta$  angle, considering a radio wave with  $Y = 0.5$ , frequency  $f = 4$  MHz, a collision frequency  $\nu = 10^5$  s<sup>-1</sup>. The curves are shown in different colours, as reported in the legend.

**Figure 4.** The graphs  $k_{ext}$ ,  $k_{ext-long}$  and  $k_{ext-long[NoDev]}$  for different values of the  $\theta$  angle, considering a radio wave with  $Y = 0.5$ , frequency  $f = 4$  MHz, a collision frequency  $\nu = 10^5$  s<sup>-1</sup>. The curves are shown in different colours, as reported in the legend.

**Figure 5.** The ray paths computed for a **1000 km** radio link, at different frequencies. The simulations are based on the eikonal equation, using an IRI derived ionosphere for June 15 at 12.00 LT, and assuming either a low ( $R_{12} = 10$ ) or a high ( $R_{12} = 100$ ) solar activity level. Both low and high ray paths can be distinguished.

1  
2  
3  
4  
5  
6  
7  
8  
9  
10  
11  
12  
13  
14  
15  
16  
17  
18  
19  
20  
21  
22  
23  
24  
25  
26  
27  
28  
29  
30  
31  
32  
33  
34  
35  
36  
37  
38  
39  
40  
41  
42  
43  
44  
45  
46  
47  
48  
49  
50  
51  
52  
53  
54  
55  
56  
57  
58  
59  
60  
61  
62  
63  
64  
65

**Figure 6.** With reference to Fig. 5, the corresponding absorption computed for the same 1000 km radio link, at different frequencies, assuming either a low ( $R_{12} = 10$ ) or a high ( $R_{12} = 100$ ) solar activity level, for both low and high ray paths. The simulations are based on general formulation, a more refined QL approximation and the usually employed non-deviative absorption.

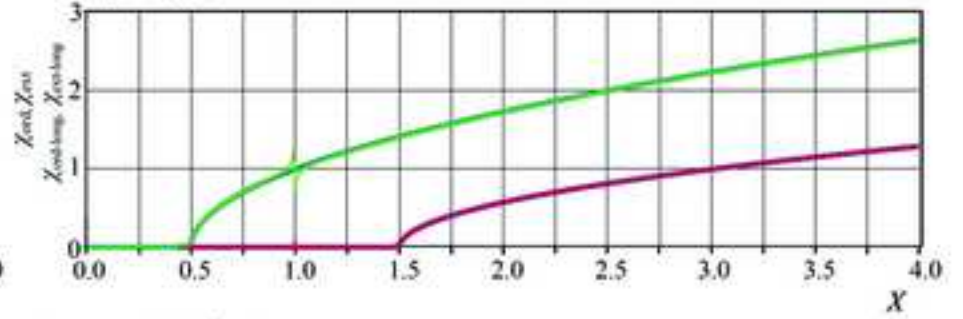




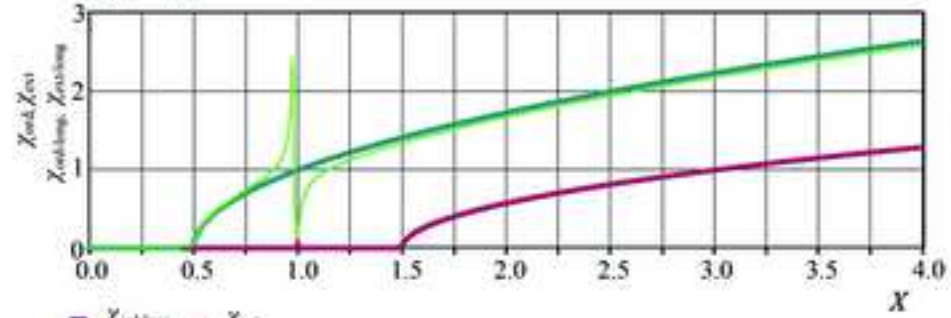
a)  $\alpha_x = 1.91 \cdot 10^3 \text{ rad/s}$   
 $\theta = 1^\circ$   
 $\alpha_x/\nu = 0.0191$



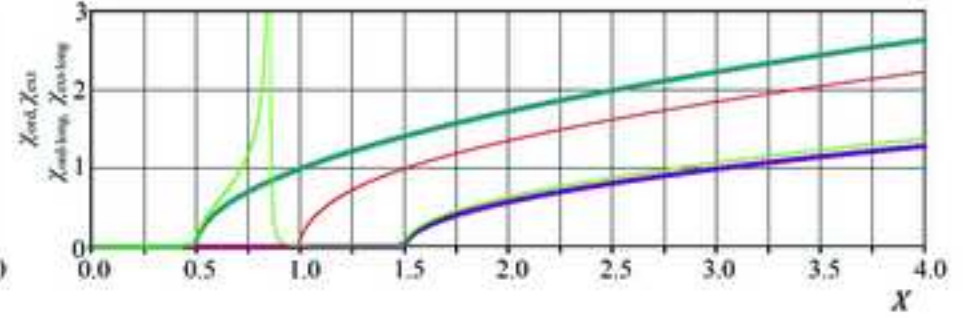
b)  $\alpha_x = 4.79 \cdot 10^4 \text{ rad/s}$   
 $\theta = 5^\circ$   
 $\alpha_x/\nu = 0.479$



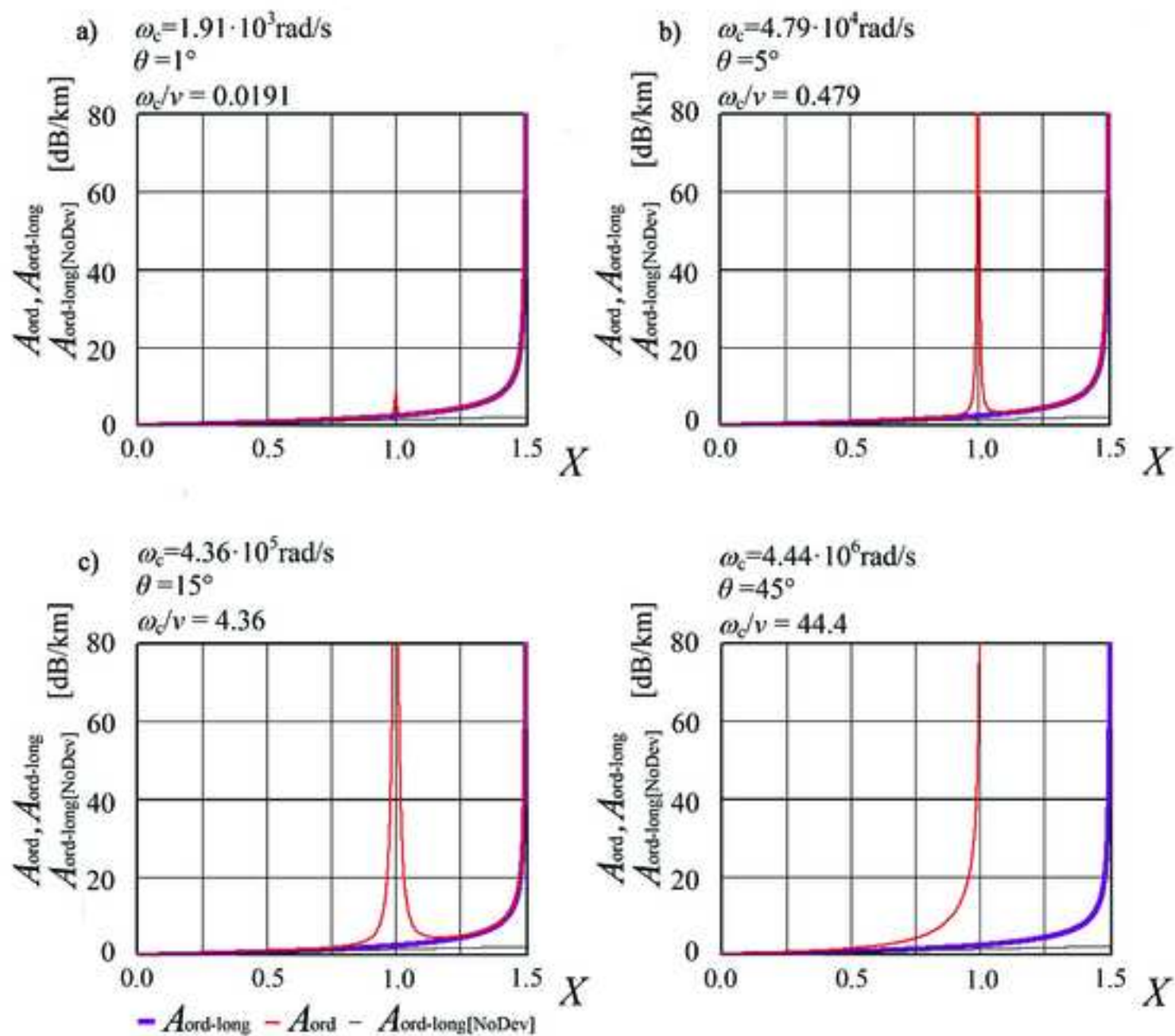
c)  $\alpha_x = 4.36 \cdot 10^5 \text{ rad/s}$   
 $\theta = 15^\circ$   
 $\alpha_x/\nu = 4.36$

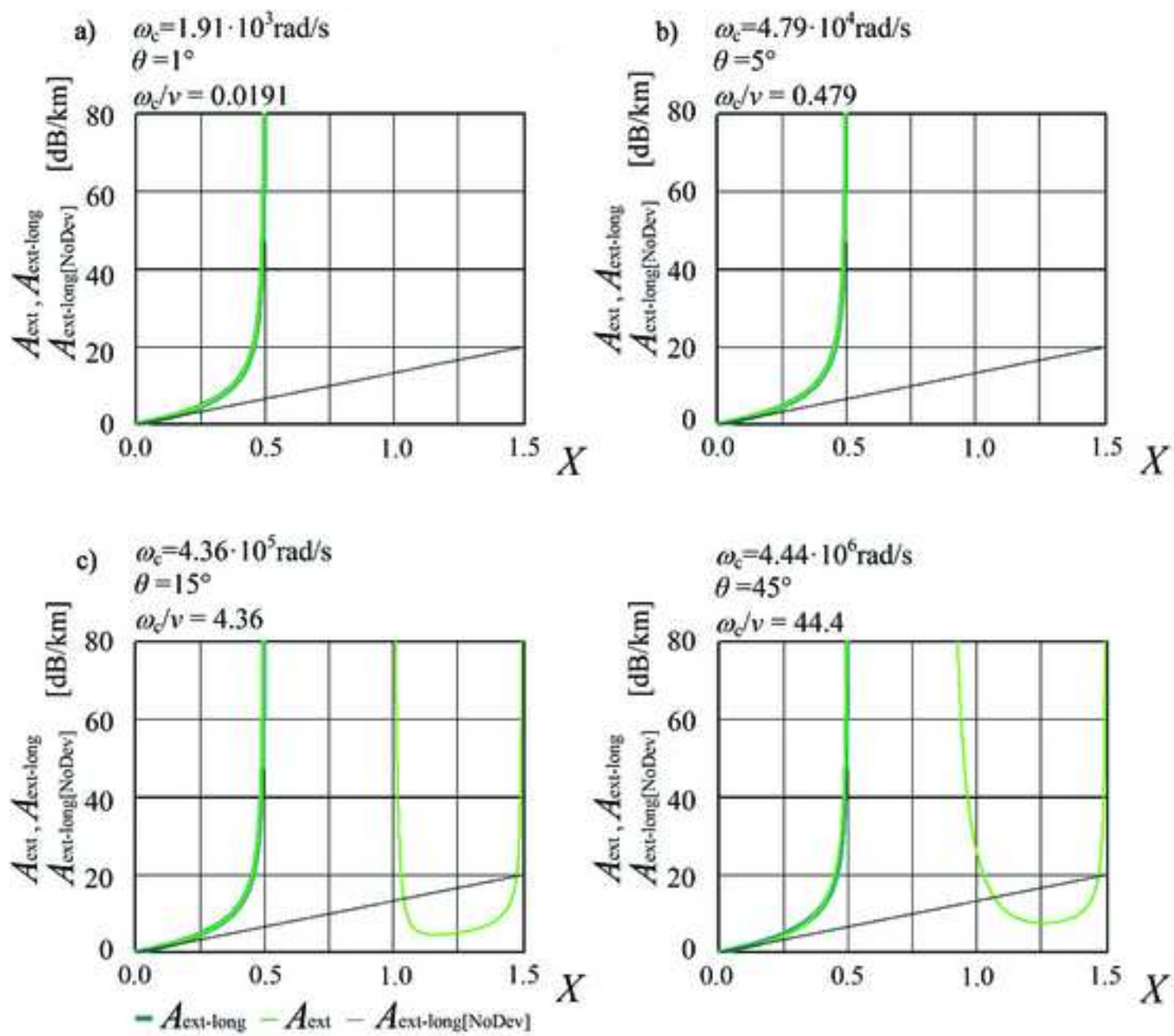


d)  $\alpha_x = 4.44 \cdot 10^6 \text{ rad/s}$   
 $\theta = 45^\circ$   
 $\alpha_x/\nu = 44.4$

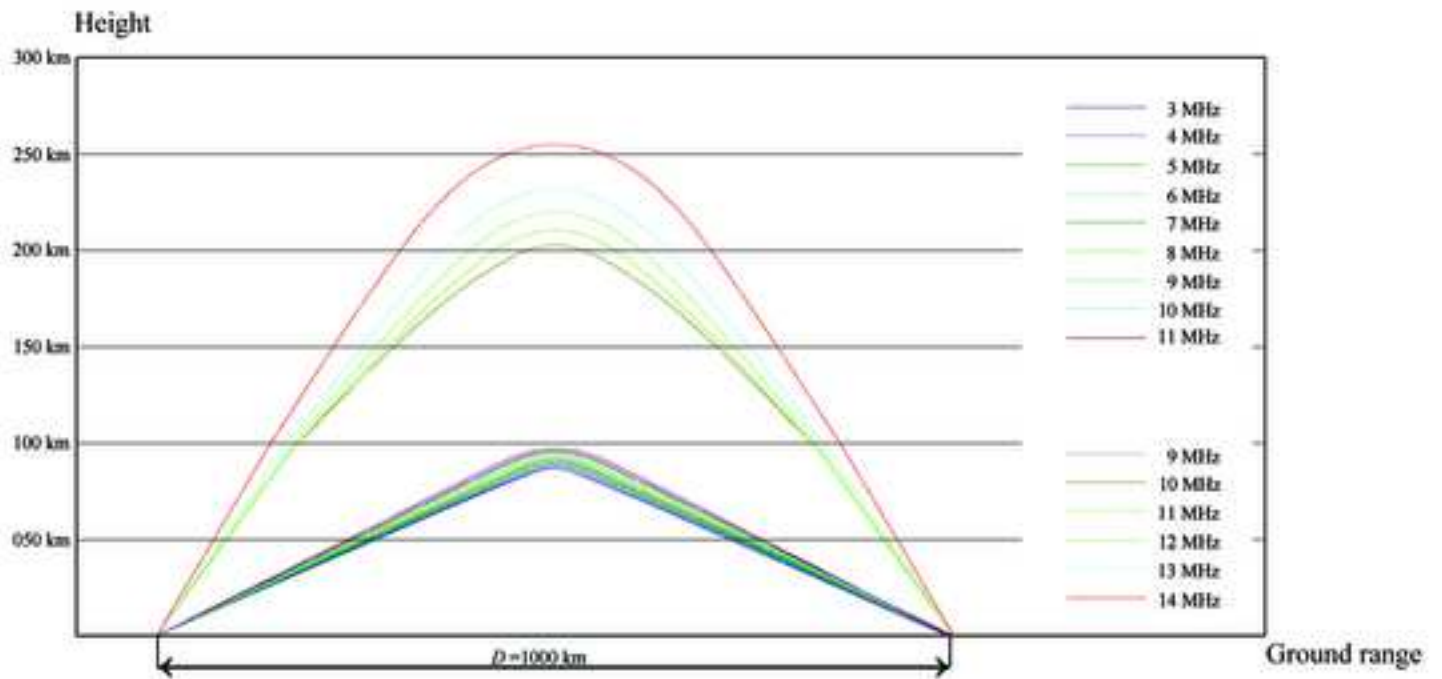


—  $Z_{ord-long} - Z_{cut}$   
—  $Z_{ord-long} - Z_{cut}$





### LOW SOLAR ACTIVITY ( $R12 = 10$ )



### HIGH SOLAR ACTIVITY ( $R12 = 100$ )

